

# Selective degradation of splicing factor CAPER $\alpha$ by anticancer sulfonamides

Taisuke Uehara<sup>1\*</sup>, Yukinori Minoshima<sup>1</sup>, Koji Sagane<sup>1</sup>, Naoko Hata Sugi<sup>1</sup>, Kaoru Ogawa Mitsuhashi<sup>1</sup>, Noboru Yamamoto<sup>1</sup>, Hiroshi Kamiyama<sup>1</sup>, Kentaro Takahashi<sup>1</sup>, Yoshihiko Kotake<sup>1</sup>, Mai Uesugi<sup>1</sup>, Akira Yokoi<sup>1</sup>, Atsushi Inoue<sup>1</sup>, Taku Yoshida<sup>1</sup>, Miyuki Mabuchi<sup>2</sup>, Akito Tanaka<sup>2</sup> & Takashi Owa<sup>3\*</sup>

**Target-protein degradation is an emerging field in drug discovery and development. In particular, the substrate-receptor proteins of the cullin-ubiquitin ligase system play a key role in selective protein degradation, which is an essential component of the anti-myeloma activity of immunomodulatory drugs (IMiDs), such as lenalidomide. Here, we demonstrate that a series of anticancer sulfonamides NSC 719239 (E7820), indisulam, and NSC 339004 (chloroquinoxaline sulfonamide, CQS) induce proteasomal degradation of the U2AF-related splicing factor coactivator of activating protein-1 and estrogen receptors (CAPER $\alpha$ ) via CRL4<sup>DCAF15</sup> mediated ubiquitination in human cancer cell lines. Both CRISPR-Cas9-based knockout of DCAF15 and a single amino acid substitution of CAPER $\alpha$  conferred resistance against sulfonamide-induced CAPER $\alpha$  degradation and cell-growth inhibition. Thus, these sulfonamides represent selective chemical probes for disrupting CAPER $\alpha$  function and designate DCAFs as promising drug targets for promoting selective protein degradation in cancer therapy.**

Protein metabolism, including protein ubiquitination and proteasomal degradation, has recently been discovered to be an important therapeutic modality for cancer. The proteasome inhibitor bortezomib has shown significant efficacy in the treatment of multiple myeloma, and the protein NEDDylation inhibitor MLN4924 is in clinical trials<sup>1–3</sup>. Furthermore, the myeloma drug lenalidomide (Supplementary Results, Supplementary Fig. 1) was reported to target cereblon (CRBN), a DDB1- and CUL4-associated factor (DCAF), and induce selective degradation of the Ikaros family zinc finger proteins 1 and 3 (IKZF1 and IKZF3) and casein kinase 1 $\alpha$  (CK1 $\alpha$ ) as key mechanisms of anticancer activity in multiple myeloma cells and in the deletion 5q (del (5q)) subtype of myelodysplastic syndrome (MDS)<sup>4–11</sup>. CRBN and other DCAFs are components of the CUL4-RING ubiquitin ligase (CRL4) complex and play a central role in substrate recognition for ubiquitination<sup>12–14</sup>. Furthermore, recent reports show that conjugation of the phthalimide moiety of thalidomide with a competitive antagonist of BET bromodomains induces degradation of the transcriptional coactivator BRD4 via CRL4<sup>CRBN</sup>, suggesting that CRBN-based target-protein degradation may also be applicable to substrate proteins other than IKZF1 and IKZF3, and thus could provide an accessible therapeutic strategy using chemical conjugation techniques<sup>15–19</sup>.

Here, we initiated a target identification study for the series of anticancer sulfonamides NSC 719239 (E7820, **1**), indisulam (**2**), and NSC 339004 (chloroquinoxaline sulfonamide, CQS, **3**) (Fig. 1a) based on observations that they may have clinical activity in cancer patients<sup>20–22</sup>. CQS and indisulam are chlorinated heterocyclic sulfonamide derivatives and have unique mean-graph fingerprints in an NCI COMPARE analysis that are quite different from those of other anticancer drugs in clinical use ([https://dtp.cancer.gov/databases\\_tools/compare.htm](https://dtp.cancer.gov/databases_tools/compare.htm))<sup>23</sup>, whereas E7820 has been shown to be a novel anticancer and antiangiogenesis agent that inhibits VEGF- or FGF-2-induced tube formation of human umbilical endothelial cells (HUVEC)<sup>24</sup>. Although these sulfonamides have been the focus of drug discovery and development efforts over the past two decades, their primary target molecule and precise mechanisms of

action remain unclear<sup>25–27</sup>. We recently found that an indisulam-resistant clonal cancer cell line was cross-resistant to E7820 and CQS but not to doxorubicin and paclitaxel (Supplementary Fig. 2)<sup>25</sup>. This suggests that the drug resistant mechanism is independent of P-glycoprotein-based multi-drug resistance and associated with a mechanism of anticancer action that is common in these three sulfonamides.

In the present study, we report that E7820, indisulam, and CQS promote selective degradation of the U2AF-related splicing factor CAPER $\alpha$  by inducing protein complex assembly between CAPER $\alpha$  and CRL4<sup>DCAF15</sup>. A single amino acid substitution of CAPER $\alpha$  conferred resistance against sulfonamide-induced CAPER $\alpha$  degradation and cell-growth inhibition, suggesting that CAPER $\alpha$  degradation is a key biochemical activity that underlies the anticancer properties of these compounds.

## RESULTS

### Downregulation of CAPER $\alpha$ by E7820, indisulam, and CQS

To clarify the cellular effect of E7820 at an early time point, we used the label-free quantitative proteome analysis strategy data-independent acquisition (DIA)<sup>28</sup>. In traditional data-dependent acquisition (DDA) with a certain isobaric labeling technique, a mass spectrometer randomly samples detectable peptides for fragmentation, often resulting in insufficient reproducibility. In DIA, all precursor ions are systematically fragmented with defined *m/z* windows, allowing highly reproducible quantification of peptides. Differential profiling of the cellular proteins in cells treated with E7820 and DMSO demonstrated that there were significant decreases in CAPER $\alpha$  in both the human colon colorectal carcinoma cell line HCT116 and the human myelogenous leukemia cell line K562 by 6 h after treatment (Fig. 1b, Supplementary Fig. 3, Supplementary Data Set 1). *In vitro* staining of HCT116 cells showed that CAPER $\alpha$  co-localizes with SC35 in the nuclear speckle, as previously reported<sup>29</sup>, and that there is a clear reduction in the CAPER $\alpha$  signal following E7820 treatment (Fig. 1c). We then compared the effects of E7820, indisulam, and CQS on CAPER $\alpha$  protein expression by performing

<sup>1</sup>Eisai Co., Ltd., Tokodai, Tsukuba-shi, Ibaraki, Japan. <sup>2</sup>School of Pharmacy, Hyogo University of Health Sciences, Minatojima, Chuo-ku, Kobe-shi, Hyogo, Japan. <sup>3</sup>Eisai Inc., Woodcliff Lake, New Jersey, USA. \*e-mail: t3-uehara@hhc.eisai.co.jp or takashi\_owa@91.alumni.u-tokyo.ac.jp.

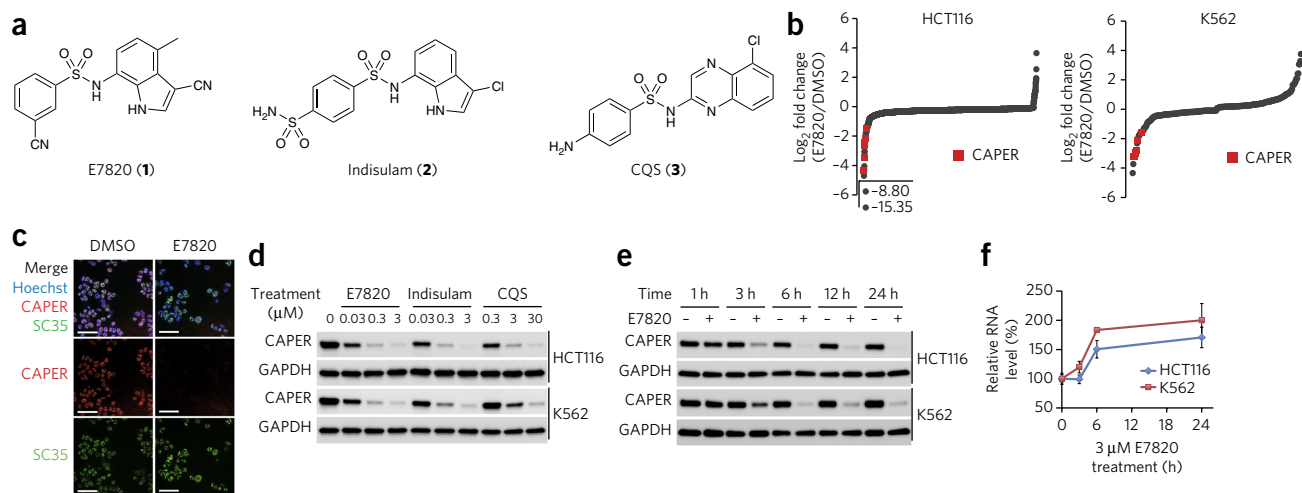


**Figure 1 | Downregulation of CAPER $\alpha$  by E7820, indisulam, and CQS.** (a) Chemical structures of anticancer sulfonamides E7820, indisulam, and CQS. (b) Proteome-wide analysis of HCT116 and K562 cells treated with 3  $\mu$ M E7820 or DMSO alone for 6 h. Each point represents the  $\log_2$  ratio of mean tryptic peptide ion peaks in E7820- versus DMSO-treated cells ( $n = 3$ ,  $P < 0.05$ , Welch's  $t$ -test). Results are representative of two independent experiments (Supplementary Fig. 3). (c) *In vitro* cell staining of HCT116 cells treated with 3  $\mu$ M E7820 or DMSO for 22 h. Scale bars, 50  $\mu$ m. Results are representative of two independent experiments. (d) Immunoblot analysis of HCT116 and K562 cells treated with the indicated concentrations of E7820, indisulam, CQS, or DMSO ("0") for 24 h. Results are representative of three immunoblot analyses. (e) Time course of CAPER $\alpha$  protein levels and (f) mRNA levels in HCT116 and K562 cells treated with 3  $\mu$ M E7820 or DMSO. GAPDH was used as the loading control. Immunoblot results are representative of two independent experiments. qPCR data are presented as the mean  $\pm$  s.d. ( $n = 3$ ). Full blot images for d and e are shown in Supplementary Figure 20.

immunoblot analysis to confirm that the reduction of CAPER $\alpha$  is a common biochemical consequence among these molecules. There was a good correlation between the extent of CAPER $\alpha$  reduction and cell-growth inhibition for all three sulfonamides (Fig. 1d, Supplementary Table 1). A qPCR assay further demonstrated that

the mRNA expression of CAPER $\alpha$  (also known as *RBM39*) increased following protein reduction in both HCT116 and K562 cells (Fig. 1e,f), suggesting that protein downregulation by these sulfonamides is post-transcriptional, and the gene expression of CAPER $\alpha$  may be negatively regulated by CAPER $\alpha$  protein.

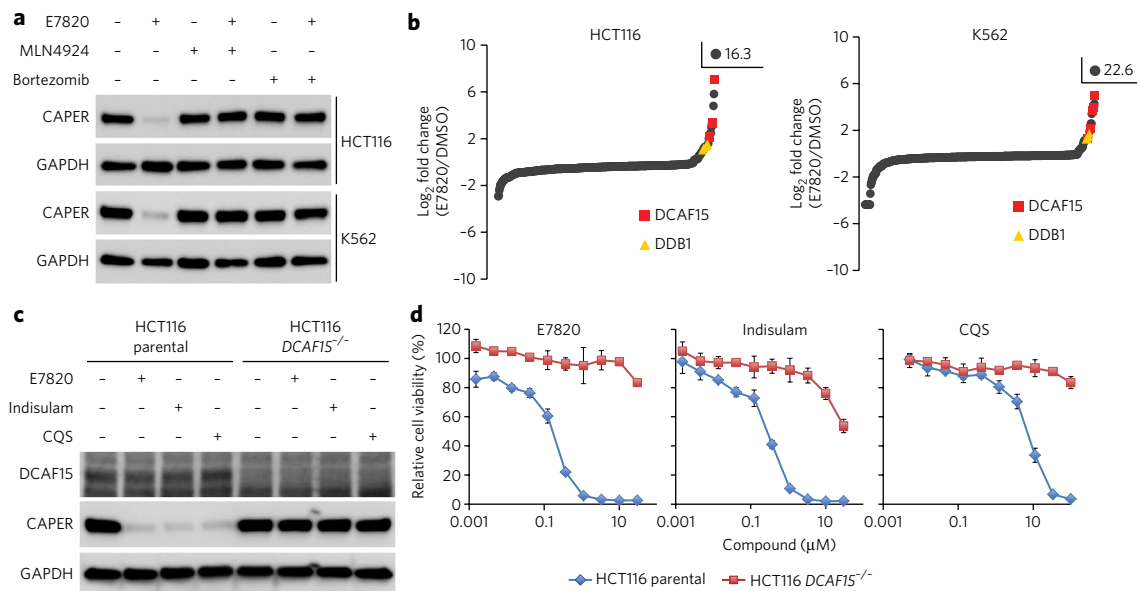


**Figure 2 | E7820, indisulam, and CQS promote CRL4<sup>DCAF15</sup> mediated CAPER $\alpha$  degradation.** (a) Chemical rescue of CAPER $\alpha$  degradation in HCT116 and K562 cells treated with 3  $\mu$ M E7820 or DMSO for 6 h. Cells were pretreated with MLN4924 (1  $\mu$ M) or bortezomib (0.2  $\mu$ M) before the addition of E7820. Results are representative of two independent experiments and biologically duplicate analysis for HCT116 and K562 cells, respectively. (b) CAPER $\alpha$  interaction analysis of HCT116 and K562 cells treated with E7820 (1  $\mu$ M) or DMSO for 6 h. Each point represents the  $\log_2$  ratio of the mean tryptic peptide ion peak following CAPER $\alpha$  co-immunoprecipitation in E7820- versus DMSO-treated cells ( $n = 3$ ,  $P < 0.05$ , Welch's  $t$ -test). Results are representative of two independent experiments. (c) Immunoblot analysis of parental and DCAF15 knockout clones of HCT116 cells treated with E7820 (3  $\mu$ M), indisulam (3  $\mu$ M), CQS (30  $\mu$ M), or DMSO alone for 6 h. Results are representative of two independent experiments. (d) Growth inhibitory curves of anticancer sulfonamides in parental and DCAF15<sup>-/-</sup> HCT116 cells. Data are presented as the mean  $\pm$  s.d. ( $n = 3$ ). Full blot images for a and c are shown in Supplementary Figure 21.

**CAPER $\alpha$  degradation depends on CRL4<sup>DCAF15</sup>**

To examine whether this sulfonamide-induced CAPER $\alpha$  reduction is dependent on cullin–RING ubiquitin ligase (CRL), we assessed the effect of MLN4924, a small-molecule inhibitor of NEDD8-activating enzyme, on protein reduction, since CRL activity depends on NEDDylation<sup>2</sup>. We found that MLN4924 completely blocked E7820-induced reduction of CAPER $\alpha$ , as did the myeloma drug bortezomib, a selective proteasome inhibitor (Fig. 2a), indicating that E7820 induces CRL-mediated ubiquitination and proteasomal degradation of CAPER $\alpha$ . Therefore, we hypothesized that these sulfonamides induce a protein–protein interaction between CAPER $\alpha$  and the CRL complex.

To identify the binding partner of CAPER $\alpha$ , we used CAPER $\alpha$  immunoprecipitation followed by DIA. Differential proteome analysis demonstrated that E7820 enhances the ability of CAPER $\alpha$  to bind to DCAF15 and DDB1 in both HCT116 and K562 cells (Fig. 2b, Supplementary Data Set 2). DDB1 functions as a linker between the CUL4 scaffolds and DCAF substrate receptors to build the CRL4 complexes, which regulate diverse protein ubiquitination and cellular functions<sup>13,14</sup>. To confirm whether DCAF15–DDB1 plays a key role in CAPER $\alpha$  degradation, we performed an siRNA-mediated knockdown of *DCAF15* and *DDB1* in HCT116 cells. As expected, both *DCAF15* and *DDB1* knockdowns rescued sulfonamide-induced CAPER $\alpha$  degradation and inhibition of cell growth in HCT116 cells (Supplementary Fig. 4). Since DDB1 functions as a general linker protein in the CRL4 complex, we suspected that DCAF15 might be a more suitable protein target for compound mediated selective protein degradation. Therefore, we established a *DCAF15* knockout clone of HCT116 using CRISPR–Cas9-based gene editing (Supplementary Fig. 5). An immunoblot analysis and cell viability assay revealed that *DCAF15*<sup>−/−</sup> HCT116 cells were also resistant to sulfonamide-induced CAPER $\alpha$  degradation and cell-growth inhibition despite strong growth inhibition caused by other cytotoxic agents (Fig. 2c,d, Supplementary Fig. 6). Unfortunately, we were unable to identify the cullin protein(s) because there were insufficient differences between compound-induced interactions and nonspecific binding of cullin protein under these immunoprecipitation conditions. Therefore, we next assessed the effect of *CUL4A* and/or *CUL4B* knockdown on CAPER $\alpha$  degradation. Interestingly, the double knockdown of *CUL4A* and *CUL4B* prevented E7820-induced CAPER $\alpha$  degradation to a significant degree, whereas the single knockdown of either *CUL4A* or *CUL4B* did not (Supplementary Fig. 7), indicating that *CUL4A* and *CUL4B* may be involved in DCAF15–DDB1-mediated protein ubiquitination in a redundant manner<sup>14,30</sup>.

**DCAF15 is the primary target of anticancer sulfonamides**

The stable transfection of *DCAF15* into *DCAF15*<sup>−/−</sup> HCT116 clonal cells successfully restored the E7820-induced protein degradation (Supplementary Fig. 8). Therefore, we examined the identity of the molecular complex that includes E7820, CAPER $\alpha$ , DCAF15, and DDB1 using *DCAF15*- or mock-vector-transfected *DCAF15*<sup>−/−</sup> HCT116 cells. Immunoprecipitation with the anti-CAPER $\alpha$  antibody followed by immunoblot analysis confirmed that E7820 induces protein complex assembly between CAPER $\alpha$  and DCAF15–DDB1. The antibody did not pull down DDB1 in the mock-transfected cells but did in the *DCAF15*-transfected cells following E7820 treatment, indicating that DDB1 binds to CAPER $\alpha$  via DCAF15 (Fig. 3a). In addition, CAPER $\alpha$  immunoprecipitation followed by a ubiquitin immunoblot analysis confirmed that E7820-induced CAPER $\alpha$  ubiquitination is dependent on DCAF15 (Fig. 3b). Next, we immunoprecipitated CAPER $\alpha$  from HCT116 cells treated with tritium-labeled-E7820 ([<sup>3</sup>H]E7820, 4, Supplementary Fig. 1) with or without cold (unlabeled) E7820 competition. The anti-CAPER $\alpha$  antibody captured a strong tritium count from the *DCAF15*-transfected cells but not from the mock-transfected or

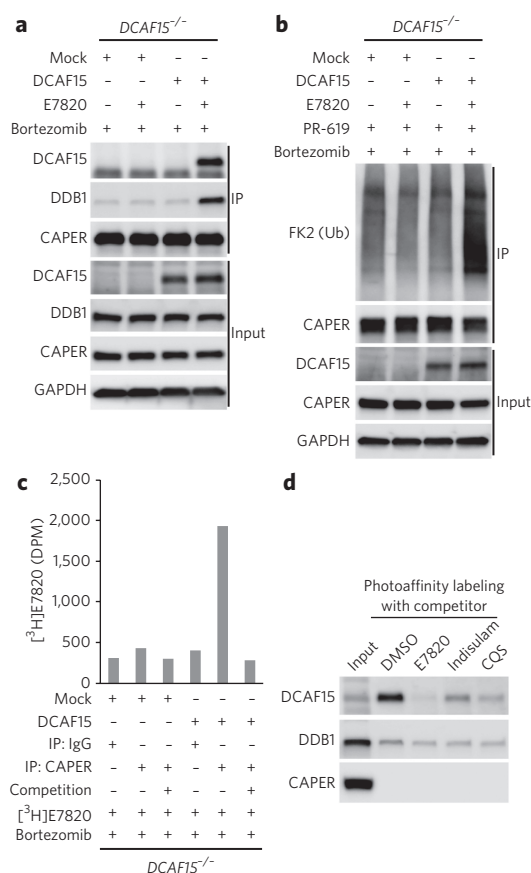


**Figure 3 | DCAF15 is the primary target of E7820, indisulam, and CQS in the ubiquitination of CAPER $\alpha$ .**

(a) Immunoprecipitation and immunoblot analysis of the CAPER $\alpha$  binding protein. Cells were pretreated with bortezomib (0.5  $\mu$ M) before treatment with E7820 (3  $\mu$ M) or DMSO alone for 3 h. IP, immunoprecipitation with anti-CAPER $\alpha$  antibody. Results are representative of two independent experiments. (b) Cell-based ubiquitination analysis of endogenous CAPER $\alpha$ . Cells were pretreated with bortezomib (0.5  $\mu$ M) before treatment with E7820 (3  $\mu$ M) or DMSO, and the de-ubiquitination inhibitor PR-619 (30  $\mu$ M), as indicated, for 3 h. IP, immunoprecipitation with anti-CAPER $\alpha$  antibody. Results are representative of two independent experiments. (c) [<sup>3</sup>H]E7820 pull-down by CAPER $\alpha$  immunoprecipitation. Cells were pretreated with bortezomib (0.5  $\mu$ M), and then treated with [<sup>3</sup>H]E7820 (1  $\mu$ M) for 3 h with or without cold E7820 competition (20  $\mu$ M). Data are the mean of two cycle analyses. Results are representative of three independent experiments. (d) Photoaffinity labeling of target protein with the biotinylated photoactive E7820 probe. The *DCAF15*-vector-transfected *DCAF15*<sup>−/−</sup> HCT116 cell lysate with or without competition of the sulfonamide derivatives (30  $\mu$ M) that had been incubated with the E7820 probe for 30 min followed by UV irradiation. Labeled proteins were enriched using streptavidin beads and then visualized by immunoblot analysis. Results are representative of two independent experiments. Full blot images for a, b, and d are shown in Supplementary Figure 22.

cold-E7820-competed cells, indicating that the E7820 molecule is present in the CAPER $\alpha$ –DCAF15–DDB1 complex (Fig. 3c). To identify a direct binding partner for E7820, we performed photoaffinity labeling with a biotinylated photoactive E7820 probe (5, Supplementary Fig. 1). Photoaffinity labeling followed by biotin–streptavidin affinity purification selectively captured and enriched DCAF15, with E7820, indisulam, and CQS all competing for probe binding (Fig. 3d). Together, these findings demonstrate that these three sulfonamides induce protein complex assembly between CAPER $\alpha$  and CRL4<sup>DCAF15</sup>, thereby promoting ubiquitination and

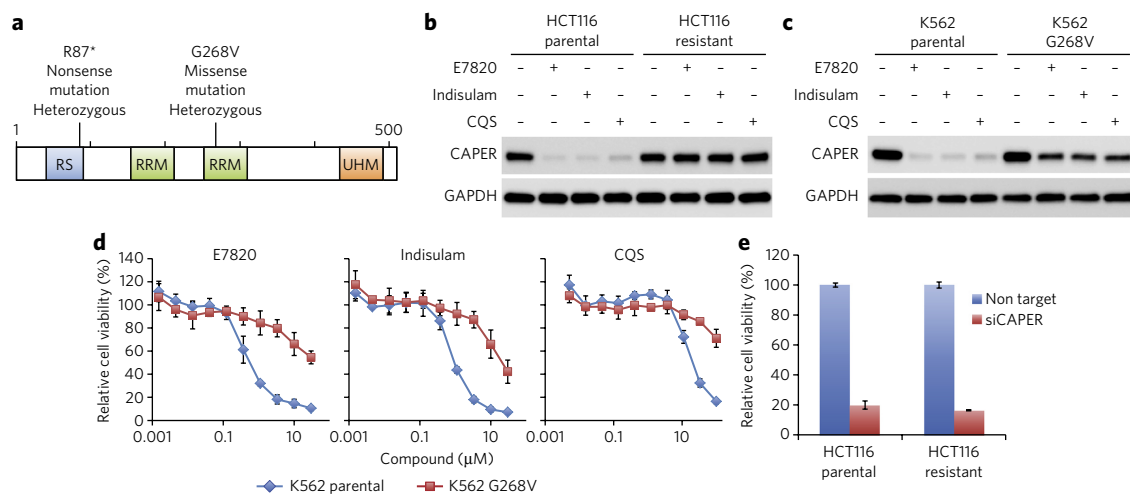


**Figure 4 | CAPER $\alpha$  degradation is a key biochemical activity that underlies the anticancer properties of E7820, indisulam, and CQS.** (a) Mapping of the CAPER $\alpha$  mutation in sulfonamide-resistant HCT116 cells. (b) Immunoblot analysis of parental and sulfonamide-resistant HCT116 cells treated with E7820 (3  $\mu$ M), indisulam (3  $\mu$ M), CQS (30  $\mu$ M), or DMSO for 6 h. Results are representative of two independent experiments. (c) Immunoblot analysis of parental and mutant K562 cells treated with E7820 (3  $\mu$ M), indisulam (3  $\mu$ M), CQS (30  $\mu$ M), or DMSO for 6 h. Results are representative of two independent experiments. (d) Growth inhibitory curves of anticancer sulfonamides in parental and mutant K562 cells. Data are presented as the mean of three independent experiments  $\pm$  s.d. (e) Effect of siRNA-mediated CAPER $\alpha$  knockdown on parental or sulfonamide-resistant HCT116 cells. Data are presented as the mean  $\pm$  s.d. ( $n = 3$ ). Full blot images for b and c are shown in **Supplementary Figure 23**.

proteasomal degradation of CAPER $\alpha$ . Moreover, the deleterious effect of DCAF15 knockdown on HCT116 cell growth indicates that the antiproliferative activities of these sulfonamides are not caused by simple antagonism toward DCAF15 (**Supplementary Fig. 4c**).

The biochemical activity of these sulfonamides might be similar to that of lenalidomide<sup>5,6</sup>. Therefore, we assessed the cross-reactivity of small-molecule-mediated protein degradation between E7820 and lenalidomide in the multiple myeloma cell line MM.1S. E7820 treatment resulted in the clear degradation of CAPER $\alpha$  but did not affect the expression of IKZF1 or IKZF3 in the MM.1S cells. By contrast, lenalidomide treatment did not decrease CAPER $\alpha$  expression at a concentration of 10  $\mu$ M, which was sufficient for IKZF1 and IKZF3 degradation (**Supplementary Fig. 9**). These results verify that the specific protein degradations of E7820 and lenalidomide are independent and not cross-reactive.

### CAPER $\alpha$ degradation is crucial for anticancer activity

We also performed differential exome sequencing of parental HCT116 cells and sulfonamide-resistant clonal cells established by serial exposure to a drug-concentration escalation procedure (**Supplementary Fig. 2**)<sup>25</sup>. We detected 17 differential gene mutations in the sulfonamide-resistant cells, including a heterozygous G268V missense mutation in CAPER $\alpha$  and a heterozygous R87\* nonsense mutation (**Fig. 4a**, **Supplementary Fig. 10**, **Supplementary Table 2**). To investigate the mutational status of the CAPER $\alpha$  protein in the sulfonamide-resistant cells, we analyzed immunoprecipitated CAPER $\alpha$  using LC-MS/MS, which demonstrated that the G268V mutant CAPER $\alpha$  was dominantly expressed in resistant cells (**Supplementary Fig. 11**). We also found that E7820 did not degrade CAPER $\alpha$  in the resistant cells (**Fig. 4b**) and did not enhance the protein-protein interaction between DCAF15–DDB1 and CAPER $\alpha$  (**Supplementary Fig. 12**). Therefore, we hypothesized that the G268V mutation confers resistance to E7820-induced CAPER $\alpha$  degradation and cell-growth inhibition. To test this hypothesis, we used CRISPR–Cas9-based gene editing to establish CAPER $\alpha$ -G268V mutant cells, which were then treated with E7820. As expected, gene sequencing revealed that the E7820 treatment enriched the G268V mutant cells in all transfectants (**Supplementary Fig. 13**). Therefore, we performed cell cloning and selected clonal cells that

had heterozygous CAPER $\alpha$ -G268V mutations for further investigation (**Supplementary Fig. 13**). Immunoblot analysis showed that K562-G268V mutant cells exhibited sulfonamide-induced incomplete degradation of CAPER $\alpha$  (**Fig. 4c**). Notably, an immunoprecipitation–LC-MS/MS analysis of CAPER $\alpha$  demonstrated that both wild-type and G268 mutant CAPER $\alpha$  proteins are coexpressed in K562-G268V mutant cells, and that only the wild-type protein is degraded by E7820, resulting in the retention of the mutant protein (**Supplementary Fig. 14**). The NMR-based solution structure of the CAPER $\alpha$  RNA recognition motif 2 (RRM2) domain reported in Protein Database (PDB 2JRS) shows that G268 is located in the alpha helix and directed outside the protein (**Supplementary Fig. 15**). Combined, this structure model and our data suggest that G268 may be a part of the degron of these sulfonamides and DCAF15 protein complex.

A cell-growth-inhibition assay indicated that the G268V mutation in CAPER $\alpha$  confers resistance to the antiproliferative activity of these sulfonamides despite strong growth inhibition by other cytotoxic agents (**Fig. 4d**, **Supplementary Fig. 16**). Compared to sulfonamide-resistant HCT116 cells, K562-G268V cells were more sensitive to these sulfonamides, which might be due to heterozygous gene editing in K562 cells (**Fig. 4d**, **Supplementary Fig. 2**). In addition, siRNA-mediated CAPER $\alpha$  knockdown resulted in significant growth inhibition not only in the parental HCT116 cells but also in the resistant clonal cells (**Fig. 4e**, **Supplementary Fig. 17**). All of these findings indicate that CAPER $\alpha$  has a critical biological function in HCT116 cell viability and the haploinsufficiency of HCT116 may render them particularly sensitive to E7820, indisulam, and CQS.

CAPER $\alpha$  is a U2AF-related splicing factor (also designated RBM39, HCC1, FSAP59, and RNPC2) that serves as a coactivator for the transcription factors AP1, ER $\alpha$ , ER $\beta$ , ERR $\alpha$ , and NF- $\kappa$ B and is involved in nuclear receptor-dependent alternative splicing<sup>29,31–35</sup>. It has previously been reported that RNAi-mediated knockdown of CAPER $\alpha$  changes the splice form of vascular endothelial growth factor A (VEGF-A)<sup>32,33,35</sup>. Here, we confirmed the modulation of VEGF-A alternative splicing via the small-molecule-induced knockdown of the CAPER $\alpha$  protein in HCT116 cells using exon-junction-targeted qPCR (**Supplementary Fig. 18**). In particular,

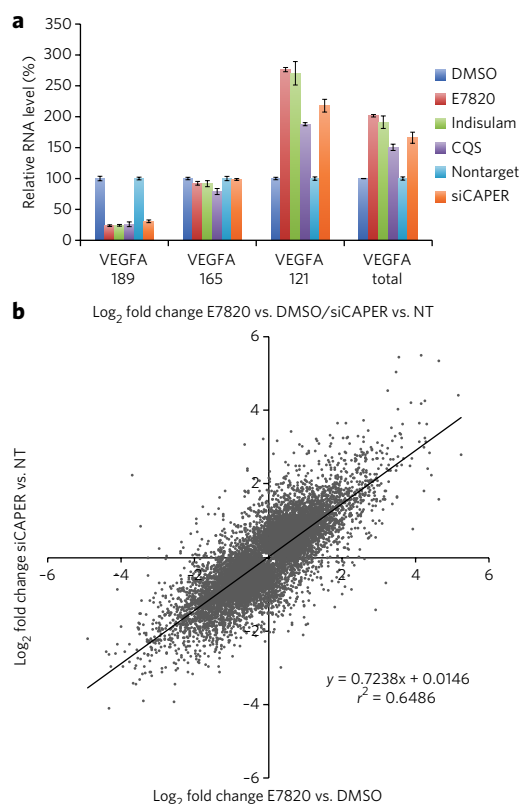


**Figure 5 | Comparison of mRNA splicing modulation and gene expression between the E7820-induced degradation and siRNA-mediated knockdown of CAPER $\alpha$ .**

(a) Exon junction targeted qPCR of VEGF-A in sulfonamide- or siRNA-treated HCT116 cells. Cells were treated with E7820 (3  $\mu$ M), indisulam (3  $\mu$ M), CQS (30  $\mu$ M), or DMSO for 24 h or with siRNA for 48 h. Data are presented as the mean  $\pm$  s.d. ( $n = 3$ ).

(b) Transcriptional comparison between the E7820-induced degradation and siRNA-mediated knockdown of CAPER $\alpha$  using DNA microarray. Cells were incubated with E7820 (1  $\mu$ M) or DMSO for 24 h or with siRNA for 48 h. Each point represents the  $\log_2$  ratio of gene expression. Data are presented as the mean of biologically triplicate analyses with Welch's  $t$ -test,  $P < 0.05$ .

we observed a significant decrease in VEGF-A-189 and a concomitant increase in VEGF-A-121 following treatment with these sulfonamides or CAPER $\alpha$  siRNA (Fig. 5a). We also undertook a comprehensive comparison of the siRNA-based genetic perturbation of CAPER $\alpha$  and the small-molecule-based chemical perturbation of the protein using microarray-based transcriptomic analysis (Fig. 5b, Supplementary Data Set 3) and confirmatory qPCR analysis (Supplementary Fig. 19), which showed that there was a high correlation ( $r^2 = 0.649$ ) between the CAPER $\alpha$  siRNA (20 nM, 48 h) and E7820 (1  $\mu$ M, 24 h) treatments. In the qPCR assay, cells treated with these sulfonamides or siRNA exhibited changes in gene expression, with two genes upregulated (*RBM15* and *ZNF177*) and four downregulated (*ITGA2*, *SLC7A11*, *GSS*, and *CCNH*) (Supplementary Fig. 19a).

## DISCUSSION

Our results demonstrate that the anticancer action of the small molecule sulfonamides E7820, indisulam, and CQS is primarily driven by assembly of a protein complex between CAPER $\alpha$  and DCAF15 that results in selective ubiquitination and degradation of CAPER $\alpha$  via CRL4<sup>DCAF15</sup>. The binding mode among the compound and proteins has yet to be fully elucidated, and in particular, additional molecule(s) not identified in this study might mediate the compound–proteins complex assembly. However, this molecular mechanism would appear to closely resemble the lenalidomide-promoted

CRBN-dependent destruction of IKZF1 and IKZF3, which results in anti-myeloma activity in the clinic. Our finding, in addition to the lenalidomide story, suggests that the drug discovery and development targeted to the ubiquitin ligase system be expanded through the identification of different substrate protein targets to be coupled with specific DCAFs by small-molecule-like IMiDs and the present anticancer sulfonamides. Therefore, in the future the structural basis of sulfonamide-induced degnon recognition by CRL4<sup>DCAF15</sup> should be clarified. In addition, CRL4<sup>DCAF15</sup> might have other substrates that were not detected in our limited proteome data sets. Further investigations of these sulfonamides as selective chemical probes may extend our understanding of the biological functions of CAPER $\alpha$ , guiding us to the selection of the right target cancer types with enhanced sensitivity to these drugs, for example, cancers with aberrant splicing that is linked to malignant transformation of cells and disease progression<sup>36</sup>.

Significantly, the putative mode of action of these sulfonamides, acting as a ‘molecular glue’, raises an implication that DCAF-dependent, small-molecule-ligand-induced selective protein degradation might have originated in a natural phenomenon, which can be promoted by primary or secondary metabolites, as exemplified by the plant hormone auxin (Supplementary Fig. 1). Auxin connects SCF<sup>TIR1</sup> ubiquitin ligase and Aux/IAA transcriptional repressors to regulate the growth and behavioral processes of plants<sup>37</sup>. Thus, our observation here might recapitulate a pharmacological example of processes that have already occurred in nature, suggesting new therapeutic possibilities through strategic chemical and pharmacologic intervention in such protein homeostasis pathways.

Received 1 August 2016; accepted 1 March 2017; published online 24 April 2017

## METHODS

Methods, including statements of data availability and any associated accession codes and references, are available in the online version of the paper.

## References

- Chen, D., Frezza, M., Schmitt, S., Kanwar, J. & Dou, Q.P. Bortezomib as the first proteasome inhibitor anticancer drug: current status and future perspectives. *Curr. Cancer Drug Targets* **11**, 239–253 (2011).
- Soucy, T.A. *et al.* An inhibitor of NEDD8-activating enzyme as a new approach to treat cancer. *Nature* **458**, 732–736 (2009).
- Kim, K.B. & Crews, C.M. From epoxomicin to carfilzomib: chemistry, biology, and medical outcomes. *Nat. Prod. Rep.* **30**, 600–604 (2013).
- Ito, T. *et al.* Identification of a primary target of thalidomide teratogenicity. *Science* **327**, 1345–1350 (2010).
- Krönke, J. *et al.* Lenalidomide causes selective degradation of IKZF1 and IKZF3 in multiple myeloma cells. *Science* **343**, 301–305 (2014).
- Lu, G. *et al.* The myeloma drug lenalidomide promotes the cereblon-dependent destruction of Ikaros proteins. *Science* **343**, 305–309 (2014).
- Fischer, E.S. *et al.* Structure of the DDB1–CRBN E3 ubiquitin ligase in complex with thalidomide. *Nature* **512**, 49–53 (2014).
- Chamberlain, P.P. *et al.* Structure of the human Cereblon–DDB1–lenalidomide complex reveals basis for responsiveness to thalidomide analogs. *Nat. Struct. Mol. Biol.* **21**, 803–809 (2014).
- Krönke, J. *et al.* Lenalidomide induces ubiquitination and degradation of CK1 $\alpha$  in del(5q) MDS. *Nature* **523**, 183–188 (2015).
- Petzold, G., Fischer, E.S. & Thomä, N.H. Structural basis of lenalidomide-induced CK1 $\alpha$  degradation by the CRL4(CRBN) ubiquitin ligase. *Nature* **532**, 127–130 (2016).
- Matyskiela, M.E. *et al.* A novel cereblon modulator recruits GSPT1 to the CRL4(CRBN) ubiquitin ligase. *Nature* **535**, 252–257 (2016).
- Jin, J., Arias, E.E., Chen, J., Harper, J.W. & Walter, J.C. A family of diverse Cul4–Ddb1-interacting proteins includes Cdt2, which is required for S phase destruction of the replication factor Cdt1. *Mol. Cell* **23**, 709–721 (2006).
- Lee, J. & Zhou, P. DCAFs, the missing link of the CUL4–DDB1 ubiquitin ligase. *Mol. Cell* **26**, 775–780 (2007).
- Hannah, J. & Zhou, P. Distinct and overlapping functions of the cullin E3 ligase scaffolding proteins CUL4A and CUL4B. *Gene* **573**, 33–45 (2015).
- Winter, G.E. *et al.* Drug Development. Phthalimide conjugation as a strategy for in vivo target protein degradation. *Science* **348**, 1376–1381 (2015).

16. Lu, J. *et al.* Hijacking the E3 ubiquitin ligase Cereblon to efficiently target BRD4. *Chem. Biol.* **22**, 755–763 (2015).
17. Zengerle, M., Chan, K.H. & Ciulli, A. Selective small molecule induced degradation of the BET bromodomain protein BRD4. *ACS Chem. Biol.* **10**, 1770–1777 (2015).
18. Bondeson, D.P. *et al.* Catalytic *in vivo* protein knockdown by small-molecule PROTACS. *Nat. Chem. Biol.* **11**, 611–617 (2015).
19. Toura, M. & Crews, C.M. Small-molecule PROTACS: new approaches to protein degradation. *Angew. Chem. Int. Edn Engl.* **55**, 1966–1973 (2016).
20. Bekaii-Saab, T.S. *et al.* A phase II study of chloroquinoxaline sulfonamide (CQS) in patients with metastatic colorectal carcinoma (MCRC). *Invest. New Drugs* **24**, 343–346 (2006).
21. Baur, M., Gneist, M., Owa, T. & Ditttrich, C. Clinical complete long-term remission of a patient with metastatic malignant melanoma under therapy with indisulam (E7070). *Melanoma Res.* **17**, 329–331 (2007).
22. Mita, M. *et al.* Phase I study of E7820, an oral inhibitor of integrin alpha-2 expression with antiangiogenic properties, in patients with advanced malignancies. *Clin. Cancer Res.* **17**, 193–200 (2011).
23. Ozawa, Y. *et al.* E7070, a novel sulphonamide agent with potent antitumour activity *in vitro* and *in vivo*. *Eur. J. Cancer* **37**, 2275–2282 (2001).
24. Funahashi, Y. *et al.* Sulfonamide derivative, E7820, is a unique angiogenesis inhibitor suppressing an expression of integrin alpha2 subunit on endothelium. *Cancer Res.* **62**, 6116–6123 (2002).
25. Yokoi, A. *et al.* Profiling novel sulfonamide antitumor agents with cell-based phenotypic screens and array-based gene expression analysis. *Mol. Cancer Ther.* **1**, 275–286 (2002).
26. Abbate, F., Casini, A., Owa, T., Scozzafava, A. & Supuran, C.T. Carbonic anhydrase inhibitors: E7070, a sulfonamide anticancer agent, potently inhibits cytosolic isozymes I and II, and transmembrane, tumor-associated isozyme IX. *Bioorg. Med. Chem. Lett.* **14**, 217–223 (2004).
27. Semba, T. *et al.* An angiogenesis inhibitor E7820 shows broad-spectrum tumor growth inhibition in a xenograft model: possible value of integrin alpha2 on platelets as a biological marker. *Clin. Cancer Res.* **10**, 1430–1438 (2004).
28. Venable, J.D., Dong, M.Q., Wohlschlegel, J., Dillin, A. & Yates, J.R. Automated approach for quantitative analysis of complex peptide mixtures from tandem mass spectra. *Nat. Methods* **1**, 39–45 (2004).
29. Imai, H., Chan, E.K., Kiyosawa, K., Fu, X.D. & Tan, E.M. Novel nuclear autoantigen with splicing factor motifs identified with antibody from hepatocellular carcinoma. *J. Clin. Invest.* **92**, 2419–2426 (1993).
30. Higa, L.A., Mihaylov, I.S., Banks, D.P., Zheng, J. & Zhang, H. Radiation-mediated proteolysis of CDT1 by CUL4-ROCI and CSN complexes constitutes a new checkpoint. *Nat. Cell Biol.* **5**, 1008–1015 (2003).
31. Jung, D.J., Na, S.Y., Na, D.S. & Lee, J.W. Molecular cloning and characterization of CAPER, a novel coactivator of activating protein-1 and estrogen receptors. *J. Biol. Chem.* **277**, 1229–1234 (2002).
32. Dowhan, D.H. *et al.* Steroid hormone receptor coactivation and alternative RNA splicing by U2AF65-related proteins CAPERalpha and CAPERbeta. *Mol. Cell* **17**, 429–439 (2005).
33. Loerch, S., Maucuer, A., Manceau, V., Green, M.R. & Kielkopf, C.L. Cancer-relevant splicing factor CAPER $\alpha$  engages the essential splicing factor SF3b155 in a specific ternary complex. *J. Biol. Chem.* **289**, 17325–17337 (2014).
34. Kang, Y.K. *et al.* CAPER is vital for energy and redox homeostasis by integrating glucose-induced mitochondrial functions via ERR- $\alpha$ -Gabpa and stress-induced adaptive responses via NF- $\kappa$ B-cMYC. *PLoS Genet.* **11**, e1005116 (2015).
35. Huang, G., Zhou, Z., Wang, H. & Kleinerman, E.S. CAPER- $\alpha$  alternative splicing regulates the expression of vascular endothelial growth factor in Ewing sarcoma cells. *Cancer* **118**, 2106–2116 (2012).
36. Sveen, A., Kilpinen, S., Ruusulehto, A., Lothe, R.A. & Skotheim, R.I. Aberrant RNA splicing in cancer; expression changes and driver mutations of splicing factor genes. *Oncogene* **35**, 2413–2427 (2016).
37. Tan, X. *et al.* Mechanism of auxin perception by the TIR1 ubiquitin ligase. *Nature* **446**, 640–645 (2007).

### Acknowledgments

T.U. thanks B.F. Cravatt, A. Fukamizu, and B.A. Littlefield for helpful advice and comments in preparing this manuscript. We thank A. Ishii and K. Tomita for technical support of the qPCR assay, M. Fukuda for support of informatics work, M. Kato for NMR analyses, and K. Kubara and M. Nakao for support of amplicon sequencing.

### Author contributions

T.U., Y.M., Y.K., T.Y., A.Y., A.T., and T.O. designed the study and experiments. T.U. performed biochemical and cell biology experiments including LC-MS/MS analysis and identified CRL4<sup>PCAF15</sup>-mediated CAPER $\alpha$  degradation. Y.M. and K.S. performed the gene sequencing and gene editing experiments and prepared the plasmid vectors. N.H.S., K.O.M., and H.K. performed biochemical and cell biology experiments. N.Y. and Y.K. prepared the chemicals. K.T. analyzed the exome sequencing data and A.I. analyzed the protein structure in PDB. M.U., T.Y., and K.O.M. performed the analyses of gene expression and RNA splicing. M.M. and A.T. established the photoaffinity labeling procedure. T.U. and T.O. interpreted experiments, directed study, and wrote the manuscript. All authors discussed results and contributed to the writing and editing of the manuscript.

### Competing financial interests

The authors declare competing financial interests: details accompany the [online version of the paper](#).

### Additional information

Any supplementary information, chemical compound information and source data are available in the [online version of the paper](#). Reprints and permissions information is available online at <http://www.nature.com/reprints>. Publisher's note: Springer Nature remains neutral with regard to jurisdictional claims in published maps and institutional affiliations. Correspondence and requests for materials should be addressed to T.U. or T.O.

## ONLINE METHODS

**Reagents.** E7820 (99.82% purity) and indisulam (E7070, 99.80% purity) were manufactured by Eisai Co. Ltd. Bortezomib, MLN4924, PR-619, and lenalidomide were purchased from LC Laboratories, Focus Biomolecules, Abcam, and BePharm Ltd., respectively. Doxorubicin and paclitaxel were purchased from Wako. All compounds were dissolved in DMSO.

**Chemistry.** CQS, tritium-labeled E7820, and biotinyl photoaffinity E7820 probes were synthesized as described in the **Supplementary Note**.

**Cell culture.** HCT116 and MM.1S cells were obtained from the American Type Culture Collection (ATCC), and K562 cells were obtained from the Health Science Research Resources Bank (HSRRB). Cells were cultured in RPMI-1640 (Wako) supplemented with 10% FBS (Sigma-Aldrich) and 1% penicillin-streptomycin (Wako), and grown at 37 °C in a humidified incubator under 5% CO<sub>2</sub>. All cell lines had been authenticated by STR profiling and confirmed mycoplasma free. Cells were treated with compounds dissolved in DMSO, and the equal amount of DMSO was added to control cells. DMSO concentrations were under 0.2%.

**Cell lysis and tryptic digestion for LC-MS/MS analysis.** HCT116 or K562 cells were plated in 10-cm inner diameter (ID) dishes and cultured for 2 days before being treated with either DMSO or 3 μM of E7820 for 6 h. The HCT116 cells were washed twice with cold PBS (Wako), lysed using 7 M UREA (Wako), 2 M Thio-UREA (Wako), 3% 3-[(3-cholamidopropyl)dimethylammonio]-1-propanesulfonate (CHAPS; Pierce), 50 mM NH<sub>4</sub>HCO<sub>3</sub> (Wako), 50 mM dithiothreitol (DTT, Pierce or Calbiochem), and cOmplete Protease Inhibitor Cocktail (Roche), and scraped onto the culture dish. The K562 cell cultures were collected and centrifuged to remove the supernatant. Cells were washed with cold PBS, centrifuged, and lysed using the same buffer as with the HCT116 cells. After removal of cellular debris by centrifugation, the total protein contents were analyzed using Pierce 660 nm Protein Assay reagent.

The protein alkylation and digestion procedure followed the Filter Aided Sample Preparation (FASP) method<sup>38</sup>, with some modification. Cell lysates of 100 μg protein were loaded on a Nanosep 10K filter unit (PALL) and centrifuged at 12,000 × *g* for 20 min at rt. The protein samples on the filter unit were washed with an 8 M UREA and 50 mM NH<sub>4</sub>HCO<sub>3</sub> solution, and carbamidomethylated with 50 mM of iodoacetamide for 20 min at rt in the dark. The iodoacetamide solutions were then removed by centrifugation and the samples were washed with an 8 M UREA/50 mM NH<sub>4</sub>HCO<sub>3</sub> solution three times. The proteins were dissolved in a 5 M UREA/50 mM NH<sub>4</sub>HCO<sub>3</sub> solution and then digested in the filter unit by 1 μg Lys-C (Wako) at 37 °C for 1 h. The samples were then diluted four-fold with 50 mM NH<sub>4</sub>HCO<sub>3</sub> solution to make 1 M UREA sample solutions that were passed through a second digestion step using 1 μg sequencing-grade trypsin (Promega) at 37 °C overnight. The digested samples were collected from the filter unit by centrifugation, following which the filters were washed twice with 8 M UREA. The samples were then acidified to make approximately 1% trifluoroacetic acid (TFA, Pierce) and desalted on an Empore solid phase extraction cartridge (C18 standard density, 3M). Peptides were eluted from the column with 80% acetonitrile/ 1% TFA, and then dried in a SpeedVac concentrator (Thermo Fisher Scientific).

**LC-MS/MS analysis.** Tryptic peptides from the whole-cell lysate or immunoprecipitation samples were reconstituted in 5% methanol/0.1% TFA and analyzed in a nano-flow LC-MS/MS system using a Q Exactive HF mass spectrometer (Thermo Fisher Scientific) coupled with an online UltiMate 3,000 Rapid Separation LC (Dionex) and an HTC PAL sample injector (CTC Analytics) fitted with a microcapillary column (360 nm outer diameter (OD) × 100 μm ID), which was packed with < 20 cm of ReproSil C18-AQ 5-μm beads (Dr. Maisch, GmbH) and equipped with an integrated electrospray-emitter tip (P-2000 laser-based puller, Sutter Instruments). Each sample was loaded onto the capillary column by 4 μL full-loop mode injection. For LC separation, a mobile phase A of 4% acetonitrile and 0.5% acetic acid (Wako) and a mobile phase B of 80% acetonitrile and 0.5% acetic acid were used for multiple linear

gradient elution from 1–37% of B over 60 min, 37–67% of B over 10 min, and 67–99% of B over 5 min, and then held at 99% of B for 10 min at 500 nL/min. The total analysis time for each sample was 120 min.

Each sample was analyzed twice using two different acquisition modes of the Q Exactive HF mass spectrometer. The first of these was DDA, which used higher energy collision dissociation (HCD) MS/MS scans (resolution 30,000) for the top 15 most abundant ions of each full-scan MS from *m/z* 350 to 1,500 (resolution 60,000) with a full-scan MS ion target of 3 × 10<sup>6</sup> ions and an MS/MS ion target of 2 × 10<sup>5</sup> ions. The maximum ion injection time for the MS/MS scans was 100 ms. The HCD normalized collision energy was set to 27, the dynamic exclusion time was set to 20 s, and the peptide match and isotope exclusion functions were enabled. The second mode was Data-Independent Acquisition (DIA), which consisted of 30 HCD MS/MS scans (resolution 30,000) with an isolation window of 27 Da (25 Da step) to cover *m/z* 350 to 1,100 and a full scan MS from 350 to 1,100. This used a full scan MS ion target of 3 × 10<sup>6</sup> ions and an MS/MS ion target of 1 × 10<sup>6</sup> ions. The maximum ion injection time for the MS/MS scans and the HCD normalized collision energy were the same as for DDA.

**LC-MS data analysis.** All DDA mass spectra were analyzed with Proteome Discoverer ver. 1.4 (Thermo Fisher Scientific) using a human Swiss-Prot database. Both MASCOT and SEQUEST-HT algorithms were used for MS/MS searching of the proteome data sets with the following parameters: oxidation of methionine and protein *N*-terminal acetylation as variable modifications, carbamidomethylation of cysteine as a fixed modification, and trypsin as the digestion enzyme. Two missed cleavages per peptide were allowed. The mass tolerance for precursor ions was set to 10 ppm, and the mass tolerance for product ions was set to 20 mDa. A maximum false discovery rate (FDR) of 1% was applied for peptide identification. Protein identification required more than two peptides per protein without protein grouping.

For the DIA data set, peptide ion peak areas were extracted and integrated using Skyline software ver 3.1.0.7382 (ref. 39). Peptide spectral libraries were established based on Thermo's MSF files using Proteome Discoverer 1.4 with a cutoff score of 0.99. The target peptide was allowed to include the following structural modifications: oxidation of methionine and protein *N*-terminal acetylation as variable modifications, carbamidomethylation of cysteine as a fixed modification, and a maximum of two missed cleavages. Transitions were set with the following conditions: precursor charges-2, 3, 4, ion charges-1, 2, ion types-y, p, product ions pick three product ions from the precursor *m/z* to the last ion, excluding the DIA precursor window, and auto-select all matching transitions. Peak areas with a maximum of seven peptides per protein were extracted from the scans within 1 min of MS/MS identification. The product ion peak areas were then summed to yield the peptide peak area, which was used for statistical analysis. The log<sub>2</sub> fold change in each peptide following E7820 treatment relative to the control value (DMSO treatment) was assessed using Welch's *t*-test (*P* < 0.05) in Excel 2010 (Microsoft).

**Antibodies.** The following antibodies were used: anti-CAPERα mouse monoclonal antibody (Santa Cruz Biotechnology, Inc, G-10, for immunoblot, 1:1000 dilution), anti-CAPERα rabbit polyclonal antibody (Bethyl Laboratories, A300-291A, for immunostaining and immunoprecipitation), anti-DCAF15 goat polyclonal antibody (Santa Cruz Biotechnology, Inc, N-16, 1:400 dilution), anti-DDB1 rabbit polyclonal antibody (Bethyl Laboratories, A300-462A, 1:2000 dilution), anti-ubiquitylated proteins mouse monoclonal antibody FK2 (HRP conjugated, Enzo Life Sciences, 1:1000 dilution), anti-Ikaros (IKZF1) rabbit polyclonal antibody (Cell signaling Technologies, #5443, 1:1000 dilution), anti-Aiolos (IKZF3) rabbit polyclonal antibody (Novus Biologicals, NBP2-24495, 1:1000 dilution), anti-GAPDH rabbit polyclonal antibody (Cell Signaling Technologies, 14C10, 1:2000 dilution), anti-vinculin mouse monoclonal antibody (Abcam, SPM227, 1:2000 dilution), normal rabbit IgG (Wako, 148-09551, for immunoprecipitation), horse anti-mouse IgG HRP conjugated antibody (Cell signaling Technologies, #7076, 1:2000 dilution), goat anti-rabbit IgG HRP conjugated antibody (Cell Signaling Technologies, #7074, 1:2000 dilution), and donkey anti-goat IgG HRP conjugated antibody (Santa Cruz Biotechnology, Inc., sc-2020, 1:4000 dilution).

**Cell immunostaining.** The cells were washed with PBS and fixed in 2% paraformaldehyde (Wako) for 30 min. The cells were then rewashed with PBS and permeabilized using 0.1% Triton X-100 for 30 min and blocked with Block Ace (DS Pharma Biomedical). The cells were incubated with anti-CAPER $\alpha$  antibody (1:2000 dilution, Bethyl Laboratories) and anti-SC-35 antibody (1:400 dilution, BD) overnight and washed with 0.05% Tween-20/Tris-buffered saline (TBS), and then labeled with Cy5-conjugated anti-rabbit IgG antibody (Invitrogen), AlexaFluor488-conjugated anti-mouse IgG antibody (Invitrogen), and Hoechst 33342 (Sigma). Image acquisition was performed using CellVoyager6000, which is an automated high-throughput cytological discovery system with laser-scanning confocal microscopes and image analysis software (Yokogawa Electric Corp., Tokyo, Japan). Three channels of excitation laser wavelengths were used (405, 488, and 635 nm) and each well was scanned with a 40 $\times$  objective to produce an image.

**Immunoblot analysis.** The cells were washed with PBS and lysed with cold Pierce RIPA buffer (Thermo Fisher Scientific) containing the cOmplete Protease Inhibitor Cocktail (Roche). After removing cell debris by centrifugation, the total protein contents were analyzed using the Pierce BCA assay. The extracts were reduced by DTT (Pierce) and separated on 4–20% SDS-polyacrylamide gradient gels (Biorad), following which the proteins were transferred to a nitrocellulose membrane (GE Healthcare Life Science) or PVDF (Biorad) membrane by electroblotting. After blocking with TBS (Takara) containing 5% non-fat dry milk (Wako) and 0.1% Tween-20 (Wako), the membrane was incubated with primary antibodies followed by horseradish peroxidase-conjugated secondary antibodies. Immunodetection was performed using Amersham ECL Prime (GE Healthcare Life Science), and a lumino-image analyzer (LAS-4000; GE Healthcare Life Science).

The DCAF15 immunoblot required some specific conditions. The cells were lysed with 4% SDS / 50 mM Tris-HCl (pH 7.5) containing the cOmplete Protease Inhibitor Cocktail (Roche). After being reduced by DTT (Pierce), the protein samples were alkylated using iodoacetamide (Wako) to block non-specific binding by the antibody. The Biorad Trans-Blot Turbo system was used for electroblotting. After blocking with TBS (Takara) containing 5% non-fat dry milk (Wako) and 0.1% Tween-20 (Wako), the membrane was incubated with the primary antibody anti-DCAF15 (N-16, Santacruz) in Can Get Signal solution 1 (Toyobo Life Science Department) at 4 °C overnight. Can Get Signal solution 2 was also used for the second antibody incubation.

**Co-immunoprecipitation of CAPER $\alpha$ .** Cells were plated in 10-cm ID dishes at a density of  $2 \times 10^6$  cells and incubated for 2 days. The cells were then pretreated with bortezomib for 30 min, following which E7820 or DMSO was added. After 3 h incubation, the cells were washed twice with cold PBS and lysed with 0.25 M sucrose (Wako), 0.3 mM sodium diethyldithiocarbamate trihydrate (Wako), 1 mM CaCl<sub>2</sub> (Wako), 1 mM MgCl<sub>2</sub> (Wako), 0.5  $\mu$ M FeCl<sub>3</sub> (Merck), 0.1% PBS, 25 mM Tris-HCl (pH 7.5) (Nippongene), cOmplete Protease Inhibitor Cocktail EDTA-free (Roche) lysis buffer in a culture dish. The cell lysates were collected and sonicated using an Astrason Ultrasonic Processor (MISONIX) and centrifuged at  $12,000 \times g$  for 20 min at 4 °C to remove any insoluble material. Protein A/G agarose beads (Pierce) and the anti-CAPER $\alpha$  antibody were incubated in lysis buffer at 4 °C, and then added to the cell lysates and incubated overnight at 4 °C in an end-over-end shaker. Following incubation, the samples were centrifuged at  $2000 \times g$  for 1 min at 4 °C to remove the supernatant, and the beads were then washed with sucrose buffer three times. The washed beads were extracted using 8 M UREA, 50 mM NH<sub>4</sub>HCO<sub>3</sub>, 50 mM DTT solution followed by the FASP protocol described in the previous section. For immunoblotting, the beads were extracted using 10% SDS, gel loading buffer (Biorad), 50 mM DTT (Pierce).

**Cell-based ubiquitination assay.** DCAF15- or mock-vector-transfected DCAF15<sup>-/-</sup> HCT116 cells were plated in 10-cm ID dishes at a density of  $2 \times 10^6$  cells and incubated for 2 days. The cells were then pretreated with bortezomib for 30 min, following which PR-619 (30  $\mu$ M) and either DMSO or E7820 (3  $\mu$ M) were added. After 3 h incubation, the cells were washed twice with cold PBS and lysed in 1 mL of cold Pierce RIPA buffer containing the cOmplete(R) Protease Inhibitor Cocktail and PR-619 (30  $\mu$ M). The cell lysates were then

sonicated in an ice-cold bath and frozen at –80 °C. The thawed cell lysates were again sonicated in an ice-cold bath and centrifuged at  $12000 \times g$  for 20 min at 4 °C to remove any insoluble material. Protein A/G agarose beads (Pierce) and anti-CAPER $\alpha$  antibody were incubated in 0.25 M sucrose-based buffer at 4 °C, and were then added to the cell lysates and incubated at 4 °C overnight in an end-over-end shaker. Following incubation, the beads were centrifuged at  $2000 \times g$  for 1 min at 4 °C to remove the supernatant, and were then washed with RIPA buffer containing protease inhibitor and PR-619 three times. The washed beads were extracted using 10% SDS, gel loading buffer (Biorad), 50 mM DTT (Pierce) for immunoblotting.

**[<sup>3</sup>H]E7820 pull-down assay.** DCAF15- or mock-vector-transfected DCAF15<sup>-/-</sup> HCT116 cells were plated in 10-cm ID dishes at a density of  $2 \times 10^6$  cells per dish and incubated for 2 days. The cells were then pretreated with bortezomib for 30 min, following which [<sup>3</sup>H]E7820 (final 1  $\mu$ M) with or without cold E7820 (final 20  $\mu$ M) were added. After 3 h incubation, cell lysis and immunoprecipitation with the anti-CAPER $\alpha$  antibody were performed using the same method as described in the previous co-immunoprecipitation section. The washed beads were extracted by boiling them in 100  $\mu$ L of SDS-PAGE sample buffer at 95 °C for 5 min. Half of each sample solution (50  $\mu$ L) was diluted with 15 mL of Hionic-Fluor (PerkinElmer) and then analyzed twice using a liquid scintillation counter (PerkinElmer Tri-Carb2100TR).

**Photo-affinity labeling using the biotinyl photoactive E7820 probe.** DCAF15-vector-transfected DCAF15<sup>-/-</sup> HCT116 cells were plated in 10-cm ID dishes at a density of  $2.5 \times 10^6$  cells and incubated for 2 days. Following incubation, the cells were washed twice with cold PBS and lysed with 0.25 M sucrose, 0.3 mM sodium diethyldithiocarbamate trihydrate, 1 mM CaCl<sub>2</sub>, 1 mM MgCl<sub>2</sub>, 0.5  $\mu$ M FeCl<sub>3</sub>, 0.1% PBS, 25 mM Tris-HCl (pH 7.5), cOmplete Protease Inhibitor Cocktail EDTA-free (Roche) lysis buffer in a culture dish. The cell lysates were collected and sonicated using an Astrason Ultrasonic Processor (MISONIX), and were then centrifuged at  $12,000 \times g$  for 20 min at 4 °C to remove any insoluble material. The biotinyl photoactive E7820 probe (0.5  $\mu$ M) was added to the cell lysates with a competitor (E7820, indinulam or CQS (30 M each), or DMSO) and then incubated for 30 min at 4 °C in an end-over-end shaker. Following incubation, the samples were irradiated with ultraviolet (UV) light for 30 s using a 365-nm cut filter, and then 10% SDS solution (final about 1%) was added. Streptavidin beads that had previously been washed were added to the sample and incubated for 2 h at rt in an end-over-end shaker. The streptavidin beads were then collected by centrifugation and washed with a 0.5% SDS, 50 mM Tris-HCl (pH 7.5) solution four times. The washed beads were extracted using 10% SDS/SDS-PAGE sample buffer, 50 mM DTT, 20 mM biotin for immunoblot analysis.

**Quantitative RT-PCR.** TaqMan Gene Expression Assays (Life Technologies) used in this study are summarized in **Supplementary Table 3**.

For time-course analysis of CAPER $\alpha$  gene expression and confirmation of siRNA-mediated knockdown, total RNA extraction and cDNA synthesis were performed using the Cell-to-CT kit (Ambion) according to the manufacturer's protocol. A quantitative PCR analysis of the cDNA (total RNA equivalent) was carried out in duplicate ( $n = 3$  biological replicates) using the TaqMan Fast Advanced Master Mix (Life Technologies) on a ViiA7 Real-time PCR System (Life Technologies). Cycle threshold (Ct) values were determined using ViiA7 software version 1.1 (Life Technologies). The relative gene expression normalized against the expression level of GAPDH was calculated using Excel 2010 (Microsoft).

For analysis of the VEGF-A splicing variant and a putative pharmacodynamic marker of CAPER $\alpha$  reduction, total RNA was prepared from HCT116 cells using RNeasy mini spin columns (Qiagen) according to the manufacturer's protocol. The yield and quality of each isolated total RNA sample was determined using a NanoDrop1000 spectrophotometer (Thermo Fisher Scientific). The cDNA synthesis was performed using a High Capacity cDNA Reverse Transcription Kit with RNase Inhibitor (Life Technologies) according to the manufacturer's instructions. Quantitative PCR analysis of the cDNA (total RNA equivalent) was carried out in duplicate ( $n = 3$  biological replicates) using the TaqMan Gene Expression Master Mix (Life Technologies) on an



ABI7900HT Real-time PCR System (Life Technologies). Cycle threshold (Ct) values were determined using SDS software version 2.2 (Life Technologies). A six-point standard curve was used to determine the PCR efficiency and relative quantitation. The relative gene expression normalized against the expression level of GAPDH was calculated using Excel 2010 (Microsoft).

**Reverse transfection of siRNA.** ON-TARGETplus siRNA and DharmaFECT 2 transfection reagent were obtained from GE Dharmacon. The siRNA used in this study are summarized in **Supplementary Table 4**.

For siRNA-mediated knockdown in HCT116 cells, 5  $\mu$ L of DharmaFECT 2 transfection reagent and 10  $\mu$ L of 20  $\mu$ M siRNA solution were mixed separately with 375  $\mu$ L Opti-MEM serum-free medium. After 5 min incubation at rt, these two solutions were mixed and incubated for more than 20 min at rt to generate a siRNA–DharmaFECT complex. Following incubation, 15  $\mu$ L or 375  $\mu$ L aliquots of the siRNA–DharmaFECT complex were added into wells of a 96-well plate or 6-well plate, respectively. Trypsinized HCT116 cells in antibiotic-free medium were then added to each well to give a final concentration of 20 nM siRNA. The cells were incubated at 37 °C in 5% CO<sub>2</sub>.

The knockdown efficacies of siRNA were assessed using qPCR or immunoblot analyses. J-011965-06 (RBM39), J-031237-18 (DCAF15), and J-012890-07 (DDB1) were then selected for further knockdown experiments.

**Plasmids for CRISPR/Cas9-based genome editing.** The CRISPR–Cas9 system used in this study was constructed by modifying previous reports<sup>40,41</sup>. The plasmid pC3-vector was constructed by deleting the SV40-Neo-pA module from the pcDNA3.1 vector (Thermo Fisher Scientific) using PCR-based mutagenesis (PrimeSTAR MAX DNA Polymerase, Clontech Laboratories Inc.). The DNA fragment coding hSpCas9-NLS was synthesized with codon-optimization by the GeneArt gene synthesis service (Thermo) and fused with the DNA fragments that code the T2A peptide sequence and the green fluorescent protein hmAzamiGreen (Amalgaam Co., Ltd.). To construct the Cas9 expression plasmid pC3-hCas9N-2A-hmAG, hSpCas9-NLS and 2A-hmAzamiGreen were subcloned into the pC3-vector. To guide RNA expression, the pMA-U6-BbsI vector was constructed. The DNA sequence of the U6 promoter-BbsI-sgRNA scaffold module was custom synthesized and subcloned into the pMA-vector by GeneArt service (Thermo). Oligonucleotides for the target sequence were synthesized, annealed, and subcloned into the BbsI site of the pMA-U6-BbsI vector.

**Plasmids for DCAF15 expression.** The piggyBac transposon vector pPBef1-mcs was constructed from the PB-EF1-MCS-IRES-GFP Vector PB530A-2 (System Biosciences Inc.) by removing 1.4 kb of the *EcoRI-SalI* fragment, which codes IRES-copGFP. The DCAF15 open reading frame (ORF) (NCBI Reference Sequence: NM\_138353) was synthesized by GeneScript. The IAG2AP module containing the IRES sequence followed by DNA encoding the hmAzamiGreen-T2A-Puromycin resistant gene was constructed using the In-Fusion method (Clontech). The EuRed ORF, which encodes the red fluorescence FusionRed protein (Evrogen) with codon modification, was synthesized by GeneArt service (Thermo). pPBef1-DCAF15-IAG2AP and the mock vector PBef1-EuRed-IAG2AP were constructed by connecting each module using the In-Fusion method.

**Transfection.** HCT116 or K562 cells were seeded at a density of  $5.0 \times 10^5$  cells per well in a six-well plate before being transfected with plasmids using Lipofectamine 3000 reagent (Thermo) the following day. Approximately 250  $\mu$ L of the transfection mixture contained 2.5–3.0  $\mu$ g of plasmid DNA, 7.5  $\mu$ L of Lipofectamine 3000, 5.0  $\mu$ L of P3000 solution, and 250  $\mu$ L OptiMEM (Thermo).

For the knockout of DCAF15, 1.0  $\mu$ g of the Cas9-plasmid and 1.0  $\mu$ g of the sgRNA-plasmid (sgRNA sequence: CTCCAGCACATAGTACAGCTTGG, where the underlined 3-bp sequence is a Protospacer Adjacent Motif (PAM) sequence) were co-transfected into HCT116 cells. At 46 h after transfection, the transfected cells were dissociated using Trypsin-EDTA solution (Wako) and mixed with the growth medium. The resuspended cells were filtered using a strainer cap tube and several hundred hmAzamiGreen positive cells were collected with a SONY SH800Z cell sorter. Following cell sorting, the transfected cells were treated and selected using 1  $\mu$ M E7820, and were then cloned

to establish DCAF15<sup>-/-</sup> HCT116 clonal cells. Knockout of the DCAF15 gene was confirmed by amplicon sequencing, as described below.

For point-mutation introduction, 1.0  $\mu$ g of the Cas9-plasmid, 1.0  $\mu$ g of the sgRNA-plasmid (sgRNA sequence: TAACTGAAGATATGCTTCGTGGG, where the underlined 3-bp sequence is a Protospacer Adjacent Motif (PAM) sequence), and 1.0  $\mu$ g of antisense donor-ssDNA (GAAGATTCATTGAAGA ACCTGGACTTACTCTTCCAAAAGGCTCAAAGATAACACGAAG CATATCTTCAGTTATGTTGAAGTGAATGAGCCACATAAA, where the underlined 3-bp sequence represents the G268V mutation site) were co-transfected into K562 cells. The transfected cells were treated and selected using 1  $\mu$ M E7820, and were then cloned to establish K562-G268V clonal cells. Introduction of the mutation was confirmed by amplicon sequencing for the genomic DNA (see below) and by immunoprecipitation/LC-MS/MS analysis for the protein.

For DCAF15 expression, following the transfection of HCT116 cells with DCAF15 and a mock vector using the piggyBac system with Lipofectamine 3000, the cells were treated and selected using 1 mg/mL puromycin. The expression of DCAF15 was then confirmed by immunoblot analysis.

**Amplicon sequencing.** Genomic DNA was extracted using the PureLink Genomic DNA Kit (Thermo) according to the manufacturer's instructions. The genomic DNA was amplified with PrimeSTAR GXL DNA Polymerase (TaKaRa Bio.) with tailed primers under the following conditions: 98 °C for 2 min, 35 cycles at 98 °C for 10 s, 55 °C for 15 s, and 68 °C for 30 s, and 68 °C for 5 min. A second PCR was then performed for indexing and adaptor addition for the Illumina platform. Here, 2  $\mu$ L of PCR products were treated with 5  $\mu$ L of ExoSAP-IT PCR Product Cleanup (USB/Affymetrix) diluted 1:10 and used as a template. This PCR was performed using NEBNext High-Fidelity 2 $\times$  PCR Master Mix (New England BioLabs) under the following conditions: 95 °C for 1 min, 30 cycles at 95 °C for 30 s, 65 °C for 30 s, and 72 °C for 3 min, and 72 °C for 5 min. The pooled samples were run on a 2% E-Gel EX Agarose Gel (Thermo) and the correct fragments were gel extracted with the NucleoSpin Gel and PCR Cleanup Kit (MACHEREY-NAGEL GmbH). Purified libraries were quantified with the QuantiFluor dsDNA System (Promega) and run on an Illumina MiSeq (Illumina Inc.).

The MiSeq sequencing run generated Illumina FASTQ files. These files were processed using in-house tools to convert the file format. Data analysis such as sequence filtering, counting reads, and visualization were performed using the TIBCO Spotfire software. The primers used in the amplicon sequencing and indexing are summarized in **Supplementary Tables 5 and 6**.

**Exome sequencing.** Genomic DNA of parental HCT116 and resistant clonal HCT116 cells were extracted and enriched using the DNeasy Blood & Tissue Kit (Qiagen) and SureSelect Human All Exon V5 (Agilent), according to the manufacturer's protocol. Whole exome sequencing was performed using a HiSeq 2000 (Illumina) with 100 base pairs on each end. The read numbers for the parental HCT116 cell line and resistant clone were 78.4 million and 94.1 million, respectively.

The reads were aligned to the reference genome sequence (GRCh37) using the Burrows-Wheeler Aligner (BWA)<sup>42</sup>. The Genome Analysis Toolkit (GATK) was used for base quality score recalibration, indel realignment, and duplicate removal<sup>43</sup>. To extract drug-resistance-associated mutations, three filters were applied to all locations on the target genome regions with mpileup base frequencies of A, T, G, and C. The first filter was a chi-squared test, which can be used to distinguish differences in base frequencies between sulfonamide-resistant and parental HCT116 cells; the cutoff value for this was set at 0.001. The second filter was a depth filter, whereby the depth of sequence coverage needed to be five or more for both samples. The final filter was a non-synonymous single nucleotide polymorphism filter, which focused on the functional changes caused by the mutations.

**Sanger sequencing.** The CAPER $\alpha$  fragment was amplified from genomic DNA using PCR primers flanking the R87\* and G268V mutations. The PCR products were treated with ExoSAP-IT (USB/Affymetrix) and sequenced directly with PCR primers. Cycle sequencing was performed using a BigDye Terminator kit, version 3.1 (Applied Biosystems). The products of the sequencing reactions

were purified using a Performa DTR Ultra 96-Well Plate Kit (Edge BioSystems) and sequenced in a 16-capillary ABI PRISM 3130xl Genetic Analyzer (Applied Biosystems).

**Transcriptional comparison using DNA microarray.** HCT116 cells were seeded in a six-well plate at a density of  $1.0 \times 10^5$  cells per well with or without the siRNA reverse transfection of the siGENOME SMARTpool of RBM39 (Dharmacon, M-011965) and non-targeting siRNA pool #2 (D-001206-14). Following incubation overnight, DMSO or E7820 was added to the siRNA-free HCT116 plate (final  $1 \mu\text{M}$  of E7820) and incubated for 24 h. Cells were then harvested using 350  $\mu\text{L}$  of Buffer RLT (Qiagen) containing 1% 2-mercaptoethanol (Nakalai tesque) either 48 h after treatment with the siRNA or 24 h after treatment with the compounds, and stored at  $-80^\circ\text{C}$  until the next step. All sample groups were prepared with three biological replicates.

Total RNA was prepared using RNeasy mini spin columns (Qiagen) according to the manufacturer's protocol. The yield and quality of each isolated total RNA sample was determined using a NanoDrop 1000 spectrophotometer (Thermo Fisher Scientific) and an RNA Nano LabChip kit analyzed on a 2100 Bioanalyzer (Agilent Technologies). NanoDrop spectrophotometers measure the absorbency at wavelengths of 280 nm and 260 nm, the ratios of which (i.e., A260:A280) are then used to assess sample purity; an A260:A280 ratio of approximately 2.0 is considered pure for RNA samples. By contrast, the 2100 Bioanalyzer calculates an RNA Integrity Number (RIN) based on the pattern of total RNA electrophoresed, which can be used as a metric for RNA degradation<sup>44</sup>; an RIN of 9.7–10.0 is considered pure for total RNA from hiPSC-derived cardiomyocytes.

Total RNA (200 ng) was converted to cyanine-3 (Cy3)-labeled complementary RNA (cRNA) using a Low Input Quick Amp Labeling Kit, One-Color (Agilent Technologies), according to the manufacturer's instructions for single-color  $8 \times 60$  K gene expression arrays. Cy3-labeled cRNAs were purified using an RNeasy Mini purification kit (Qiagen) and hybridized to the SurePrint G3 Human Gene Expression  $8 \times 60$  K Microarray (Agilent Technologies) at  $65^\circ\text{C}$  for 17 h with a Gene Expression Hybridization Kit (Agilent Technologies), according to the manufacturer's instructions. The arrays were washed with a Gene Expression Wash Pack (Agilent Technologies) and scanned on a DNA Microarray Scanner (Agilent Technologies) according to the manufacturer's instructions. The scanned images were then quantified using Feature Extraction software (version 11.5.1.1, Agilent Technologies), and the resulting files were imported and analyzed with GeneSpring (version

12.5, Agilent Technologies). The raw data were normalized using a quantile method. The differences between treatments were assessed using Welch's *t*-test, followed by an adjustment for multiple comparisons using the FDR approach (Benjamini-Hochberg procedure). A gene was considered to be differentially expressed when its absolute fold change relative to the control value was  $\geq 1.5$  with an FDR *P* value of  $\leq 0.05$ .

**Computational amino acid substitution of CAPER $\alpha$ .** <sup>268</sup>Glycine in the CAPER $\alpha$  NMR structure (PDB 2JRS) was mutated to valine, and the side chain of the mutated valine was energy minimized using CHARMM force field. Modeling and minimization was carried out using Discovery Studio 3.5 (Dassault Systemes, <http://www.3ds.com>).

**Cell viability assay.** Cells were plated in a 96-well microtiter plate with or without siRNA reverse transfection and incubated overnight. Serial dilutions of compounds were then added to each well. After 3 days, 10  $\mu\text{L}$  of WST-8 reagent (Dojindo) was added to each well. The absorbency at 450 nm (A450) was monitored and compared with a reference measurement at A660 using an EnVision 2103 Multilabel Reader (PerkinElmer), RAINBOW microplate reader (SLT Lab Instruments), or Sunrise microplate reader (TECAN).

**Data availability.** Proteome, exome sequencing, and DNA microarray data have been deposited in the jPOST (accession code: [JPOST000232](https://jpost.org/jpost/entry/JPOST000232)), NCBI (accession code: [SRP097451](https://www.ncbi.nlm.nih.gov/geo/query/acc.cgi?acc=SRP097451)), and GEO (accession code: [GSE93829](https://www.ncbi.nlm.nih.gov/geo/query/acc.cgi?acc=GSE93829)), respectively.

38. Wiśniewski, J.R., Zougman, A., Nagaraj, N. & Mann, M. Universal sample preparation method for proteome analysis. *Nat. Methods* **6**, 359–362 (2009).
39. Egerton, J.D., MacLean, B., Johnson, R., Xuan, Y. & MacCoss, M.J. Multiplexed peptide analysis using data-independent acquisition and Skyline. *Nat. Protoc.* **10**, 887–903 (2015).
40. Mali, P. *et al.* RNA-guided human genome engineering via Cas9. *Science* **339**, 823–826 (2013).
41. Cong, L. *et al.* Multiplex genome engineering using CRISPR/Cas systems. *Science* **339**, 819–823 (2013).
42. Li, H. & Durbin, R. Fast and accurate short read alignment with Burrows-Wheeler transform. *Bioinformatics* **25**, 1754–1760 (2009).
43. McKenna, A. *et al.* The Genome Analysis Toolkit: a MapReduce framework for analyzing next-generation DNA sequencing data. *Genome Res.* **20**, 1297–1303 (2010).
44. Schroeder, A. *et al.* The RIN: an RNA integrity number for assigning integrity values to RNA measurements. *BMC Mol. Biol.* **7**, 3 (2006).